Advanced L-Band SAR System Concepts for High-Resolution Ultra-Wide-Swath SAR Imaging

12 – 14 September 2017
ESA/ESTEC, Noordwijk, The Netherlands

G. Krieger[(1)], F. Queiroz de Almeida[(1)], S. Huber[(1)], M. Villano[(1)], M. Younis[(1)], A. Moreira[(1)], J. Del Castillo[(1)], M. Rodriguez Cassola[(1)], P. Prats[(1)], D. Petrolati[(2)], M. Ludwig[(2)], C. Buck[(2)], M. Suess[(2)], N. Gebert[(2)]

[(1)] German Aerospace Center (DLR), Microwaves and Radar Institute, Germany
[(2)] European Space Agency (ESA), ESTEC, Netherlands

ABSTRACT

This paper reviews multichannel SAR instrument architectures, modes and processing techniques for the imaging of ultra-wide swaths with high azimuth resolution. The review includes both direct radiating arrays and reflector-based system architectures that are operated in either a single-transmit multiple-receive (SIMO) or in a multiple-transmit multiple-receive (MIMO) mode. The work has been conducted by DLR under the ESA contract "Advanced Processing Techniques for Next Generation Multichannel SARs" with the main objective to identify suitable SAR modes, processing techniques and system architectures for the definition and design of a next generation L-band SAR with unprecedented imaging capabilities. The goal is to map an ultra-wide swath of 400 km with 5 m azimuth resolution and to achieve, at the same time, an excellent imaging quality where both the noise equivalent sigma zero (NESZ) and the distributed ambiguity ratio (DTAR) are better than -25 dB. Towards this end, a large number of different SIMO and MIMO system candidates have been identified and assessed in view of achieving the demanding performance goals.

INTRODUCTION

Synthetic aperture radar (SAR) is a well-established remote sensing technique that can provide high-resolution radar images of the Earth surface independent of weather and sunlight illumination [1]. SAR images of the Earth are now regularly acquired by an increasing number of satellites and form the basis for a wide range of remote sensing applications and services. While the performance of SAR systems has significantly evolved over the last decades, current spaceborne SAR systems are still limited in their imaging capabilities. A representative example are the Sentinel-1 a/b satellites which can acquire in their standard interferometric wide-swath (IW) mode SAR images with an azimuth resolution of 20 m at a swath width of 250 km [2]. In the extra wide-swath (EW) mode, the coverage can even be extended to 400 km at the cost of impairing the azimuth resolution to 40 m. SAR images with an improved azimuth resolution of 5 m can also be acquired in the stripmap mode (SM) by narrowing the swath width to 80 km. A further limitation is that these images can only be provided in a single- or dual-polarized SAR mode. While the state-of-the-art satellites Sentinel-1A and Sentinel-1B provide together undoubtedly a major step towards a systematic quasi-continuous observation of the Earth surface, there remain still numerous services and applications that require improved imaging capabilities like higher resolution, wider swath coverage, and full polarization [3]. Moreover, an L-band high-resolution wide-swath SAR observatory would be an ideal complement to the existing Sentinel-1 C-band SAR mission, since a number of scientific studies have proven that the longer wavelength is well suited to extract unique information products related to vegetation, soil and ice [4]. A further dimension will be opened by the interferometric combination of multiple L-band SAR images. Here, the long wavelength is well suited to penetrate vegetation and to mitigate temporal decorrelation, thereby allowing for large scale continuous deformation measurements with hitherto unparalleled resolution and coverage. Table 1 compares the specification of Sentinel-1 with the requirements of the new L-band SAR system. It becomes apparent, that the new L-band SAR shall not only increase the number of acquired resolution cells by a factor of 6.4 (32) if compared to Sentinel-1's IW (EW) mode, but it shall also improve both the noise-equivalent sigma zero (NESZ) and the distributed ambiguity ratio (DTAR) by 3 dB.

Table 1: Comparison of the Main Instrument Requirements for Sentinel-1 and the Advanced L-Band SAR

Parameter		Sentinel-1	New L-Band SAR	Comment
Orbit		12/175 (693 km)	~ 700 km	proposed orbit: 14/201 (773 km) with equatorial ground-track separation of 199.4 km for full quad-pol coverage
Centre Frequency		5.405 GHz	1.2575 GHz	longer wavelength (factor 4.3) requires larger antenna
Polarization		single, dual	single, dual, quad	reduced coverage for quad-pol mode
Swath Width	single/dual	250 km (IW), 400 km (EW)	≥ 400 km	for single- & dual-polarized modes (2 global maps/week)
	quad	not available	≥ 200 km	for quad-polarization mode (global coverage in 14 days)
Azimuth Resolution		20 m (IW), 40 m (EW)	≤ 5 m	single-look resolution
Range Resolution		5 m (IW), 20 m (EW)	≤ 5 m	single-look resolution in ground range (or 80 MHz)
NESZ		≤ -22 dB	≤ -25 dB	higher sensitivity required for L band
DTAR		≤ -22 dB	≤ -25 dB	higher distributed target-to-ambiguity ratio for L band

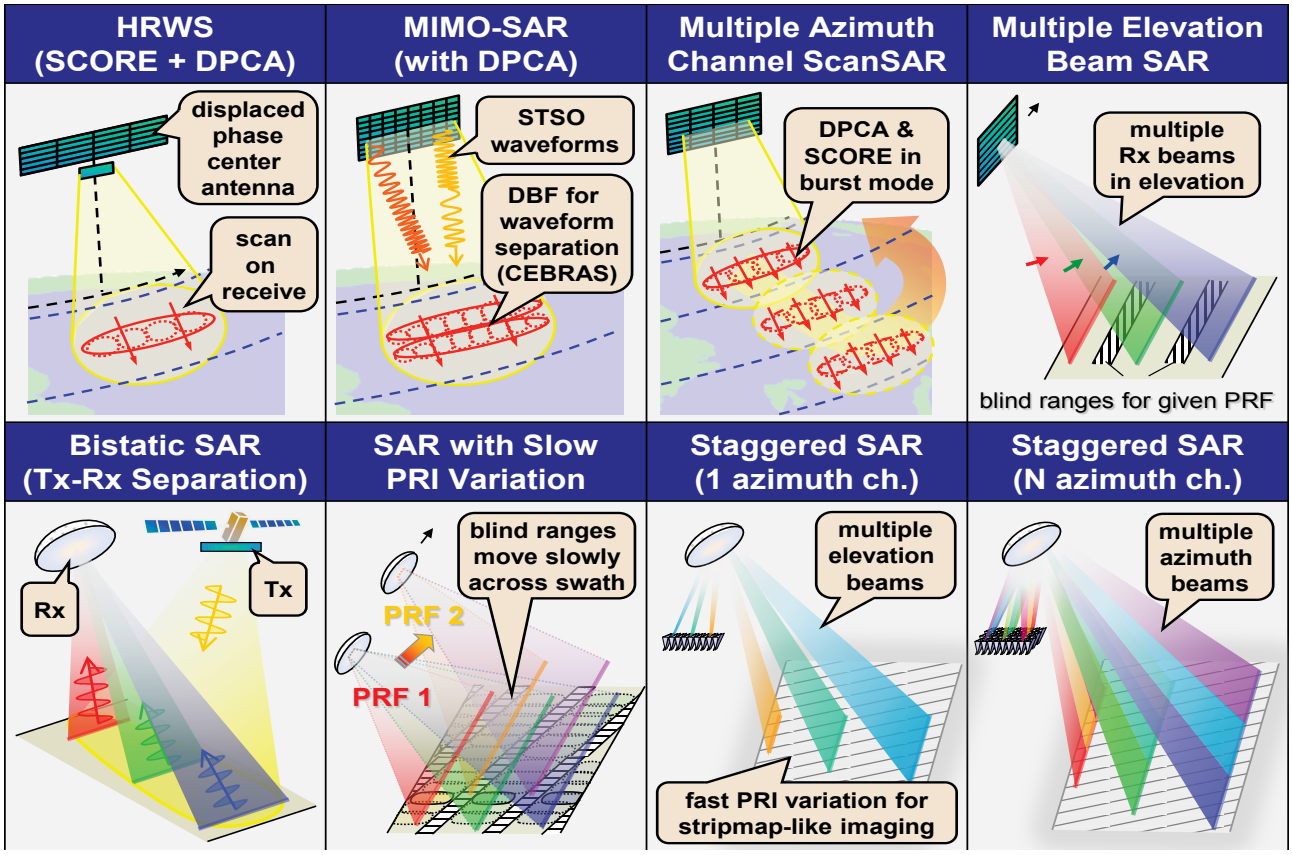

Figure 1: Concepts for high-resolution wide-swath SAR imaging (adapted from [8]). Upper row from left to right: HRWS SAR with real-time digital beamforming in elevation and multiple Rx channels in azimuth ([5], [9], [10], [11]), MIMO SAR with multiple transmit channels in azimuth ([12], [13], [14]), ScanSAR with multiple azimuth channels ([15], [16], [17], [18], [19]), SAR with multiple elevation beams ([6], [15], [21], [22], [23]). Lower row from left to right: Bistatic SAR with multiple elevation beams ([24], [15]), reflector SAR with slow PRI variation mode ([15], [8]), staggered SAR with fast PRI variation ([25], [15], [26], [27], [28], [29], [30]), staggered SAR with multiple azimuth channels ([31], [32]).

SYSTEM ARCHITECTURES AND MODES

To meet the demanding requirements of the new L-band SAR, a large number of SIMO and MIMO system architectures and imaging modes have been analysed (Figure 1 shows a subset of the analysed systems). The investigated concepts comprise multichannel SAR architectures with both direct radiating planar arrays and reflector antennas and can be distinguished according to their basic data acquisition principle. The first class employs multiple azimuth antennas and/or beams in the along-track direction [5], while the second class employs multiple beams and/or Rx channels in the elevation direction [6]. In principle, it is also possible to combine both techniques for the implementation of an advanced high-resolution wide-swath SAR imaging system [7].

Stripmap SAR with Multiple Azimuth Channels

The first system, shown in Figure 1 on the upper left, is an adaptation of the HRWS architecture proposed in [10]. This system employs a long antenna with multiple displaced antenna phase centres in azimuth to collect, for each transmitted pulse, multiple samples along the synthetic aperture [5]. In addition, digital beamforming in elevation is used to obtain a high Rx gain without losing wide swath coverage [10]. Table 2 shows that a good NESZ and a good range ambiguity performance can be achieved with a moderate Tx power and antenna height. The system requires, however, a very long antenna of 34 m, which makes the HRWS stripmap SAR more suitable for the imaging of moderate swath widths.

Table 2: Performance of HRWS Stripmap SAR with Multiple Azimuth Channels

Parameter	Value	NESZ	Range Ambiguities (RASR)	Azimuth Ambiguities (AASR)
Tx antenna	12.0 x 0.8 m^2	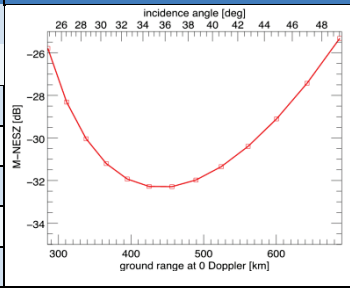	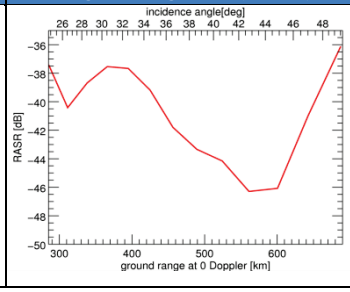	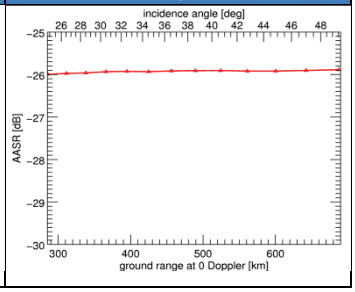
Rx antenna	34.0 x 1.1 m^2			
Orbit Alt.	700 km			
Azim. Ch.	4			
Tx Power	600 W (avg.)			
Duty Cycle	10%			
PRF	430 Hz			

MIMO-SAR with Multiple Azimuth Channels

A possible technique to reduce the antenna length is the operation in a MIMO-SAR mode where the leading and trailing edges of the antenna are used to simultaneously transmit two orthogonal pulses [12], [13], [14]. As illustrated in Figure 2, this allows for the acquisition of additional phase centres for each transmitted pulse pair. As the resulting phase centres cover, if compared to the previous DPCA approach, twice the azimuth interval this enables, for the considered swath width of 400 km, a notable reduction of the antenna length from $l_{ant} \gtrsim 35$ m to $l_{ant} \approx 20$ m. Such a value is much closer to the 15 m antenna length that has already been deployed in orbit for Radarsat-2, but it is still considered a challenge and cost driver. Moreover, a sufficient antenna height h_{ant} has to be provided to separate the short-term shift-orthogonal (STSO) waveforms by digital beamforming in elevation [12], [33], [13], [34], [14]. Assuming that the two waveforms keep their orthogonality for an interval of $\Delta\tau_{STSO} = 200$ µs (i.e. 8.5% of the pulse repetition interval for a PRF of 425 Hz) as well as an orbit height of $h_{sat} = 700$ km and a maximum incident angle of $\theta_{i,max} = 50°$, the required antenna height is approximately 10 m in L band, 2.5 m in C band, and 1.4 m in X band (cf. Figure 3). The antenna height could be reduced by increasing $\Delta\tau_{STSO}$, but this is in conflict with the required swath width and the timing diagram. To summarize, the proposed MIMO SAR may be an interesting candidate for an X- or C-band system if a very high resolution in the meter or even decimetre range is required over a swath width up to 200-300 km. Such a system allows for a transmit PRF above 600 Hz, and therefore a reduction of the antenna length to 12-15 m. The required antenna height depends on the STSO interval and therefore on both the timing diagram and the swath width. As a first approximation, antenna heights in the order of 1.5 m and 3 m should be sufficient in X and C band, respectively, to map a 250 km wide swath if an advanced range ambiguity suppression technique like CEBRAS is employed to separate the STSO waveforms [35]. The MIMO-SAR approach is, however, not considered suitable to meet the requirements of the intended ultra-wide-swath L-band system.

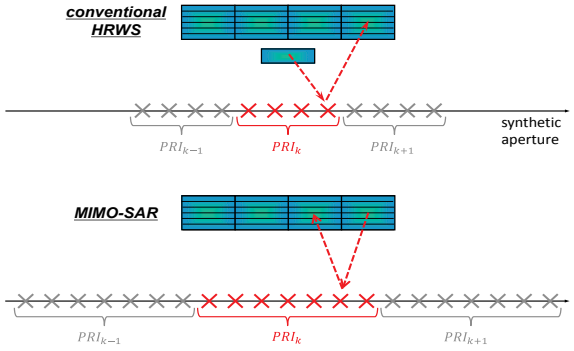

Figure 2: Additional phase centres provided by a MIMO SAR for high-resolution wide-swath SAR imaging. (Top) azimuth phase centres for a SIMO SAR where multiple displaced subapertures record the radar echoes from a single transmitter (cf. [5]). (Bottom) MIMO SAR where the left and right sub-apertures transmit short-term shift-orthogonal (STSO) waveforms that can be separated by digital beamforming on receive in elevation. The MIMO SAR provides, for each transmitted pulse, more phase centres and covers therefore a wider span of the synthetic aperture. Hence, a lower transmit PRF can be used which allows for the mapping of a wider swath.

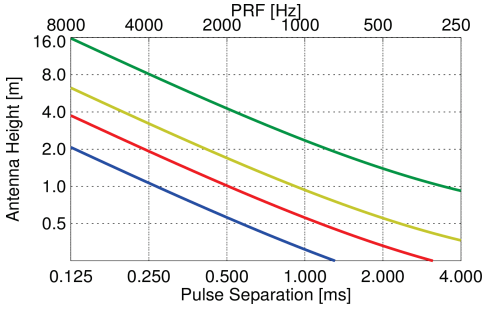

Figure 3: Minimum antenna height for L (green), S (yellow), C (red), and X (blue) band. The maximum incident angle is $\theta_{i,max} = 50°$, and the satellite height is $h_{sat} = 700$ km.

ScanSAR with Multiple Azimuth Channels

Another possibility for high-resolution ultra-wide-swath imaging is the multi-channel ScanSAR (or TOPS) mode that is illustrated in Figure 1 in the upper middle right. This mode employs multiple azimuth channels to achieve a high resolution in the along-track direction and, in addition, a ScanSAR operation to map a wide swath with a moderate antenna length [15], [16], [17], [18], [19]. Assuming an antenna length of 12 m, the minimum PRF is in the order of 1.25 kHz. A timing analysis reveals that at least 4 bursts are required to cover a 400 km swath without nadir returns. In consequence, significant variations of the Doppler centroids will be observed for different along-track positions within the SAR image. The corresponding squint angles cover an interval that may be approximated as $\Delta\psi \approx N_{burst} \cdot \lambda/2\delta_{az}$. For an L-band SAR with 5 m azimuth resolution and 4 bursts, this yields a squint angle variation of $\Delta\psi \approx 5.4°$. The high squint angles and their variations during the SAR data acquisition may have several detrimental implications for SAR imaging and SAR interferometry. Examples are a rather large range cell migration, significant variations in the line-of-sight angle for deformation and target motion measurements [36], as well as discontinuities among the burst transitions due to atmospheric propagation effects. Especially for low frequency SAR systems, the latter may become

Table 3: Performance of 3-Burst ScanSAR with Multiple Azimuth Channels and Active Nadir Suppression

Parameter	Value	NESZ	Range Ambiguities (RASR)	Azimuth Ambiguities (AASR)
Antenna	12.6 x 3.6 m^2	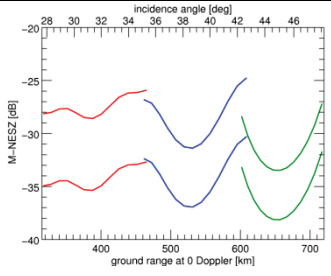	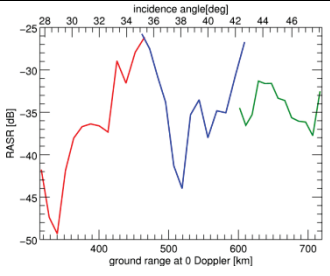	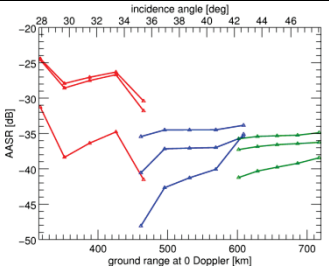
Ant. Elem.	36 x 24			
Orbit Alt.	773 km			
Azim. Ch.	6			
Tx Power	1.5 kW (avg.)			
Duty Cycle	10%			
Bursts	3			

Table 4: Performance of Bistatic SAR with Multiple Elevation Beams

Parameter	Value	NESZ	Range Ambiguities (RASR)	Azimuth Ambiguities (AASR)
Tx Antenna	10 x 0.65 m^2	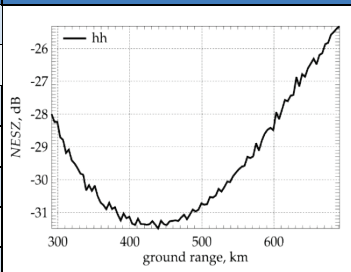	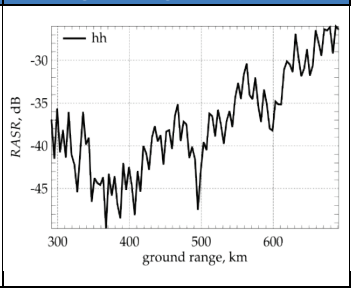	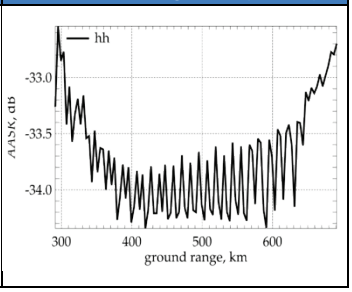
Rx Antenna	12 m ∅			
Orbit Alt.	700 km			
Elev. Ch.	45			
Tx Power	350 W (avg.)			
Losses+NF	5 dB			
Beanform.	MVDR			

an annoying error source, as it has, e.g., been shown in [37] that already rather small variations in the look angle may be associated with significant ionospheric phase disturbances. As such effects have already been observed at the burst transitions of TOPS acquisitions with TerraSAR-X and Sentinel-1A [38], and as these effects increase with both the wavelength and the squint angle difference, they may become challenging for future low frequency high-resolution ultra-wide-swath SAR systems that intend to use the multi-channel ScanSAR mode with its inherently large squint angle variations. To mitigate the squint angle variations in the multichannel ScanSAR mode, and to reduce the required number of azimuth channels, a new technique has been developed to suppress nadir echoes in SAR images by employing waveform diversity on transmit together with a dedicated dual-focusing step in the SAR processing [39]. This enables a reduction of the number of bursts from four to three, thereby reducing the number of azimuth channels from eight to six and the squint angle variation from 5.4° to 4°. The latter squint angle corresponds to burst separations of approx. 65 km at the satellite height and 30 km at an altitude of 350 km which is typical for the peak electron density in the ionosphere. Table 3 shows the predicted performance of the multichannel ScanSAR mode with three bursts.

SAR Systems with Multiple Elevation Beams

The system architectures discussed in the previous sections used multiple azimuth channels to resolve the contradicting requirements between azimuth resolution and swath width. In addition, it was implicitly assumed that these systems use also the scan-on-receive (SCORE) or SweepSAR technique which employs an enlarged elevation aperture in combination with real-time beamforming on receive to obtain a high antenna gain towards the expected direction of the arriving radar echoes [9], [20], [10], [11], [21]. As the scan-on-receive technique requires anyway multiple elevation channels, it may be worth to consider also SAR systems that form, from the received sub-aperture or feed signals, not only one, but multiple elevation beams at the same time [6]. An example for such a system is illustrated on the upper right of Figure 1. The system illuminates a wide swath with a high PRF as required to obtain a fine azimuth resolution. In consequence, the radar echoes from multiple transmitted pulses will arrive simultaneously at the radar. In a conventional SAR, these echoes would be regarded as annoying range ambiguities, but by taking advantage of the high receiving aperture and the multiple elevation channels one may form not only one, but multiple narrow elevation beams, each following the radar echo of a different transmitted pulse. By this, it becomes possible to map multiple swaths at the same time. The individual swaths are, however, separated by blind ranges, as a spaceborne radar can typically not transmit and receive at the same time. One option to avoid such blind ranges is the separation of the Tx and Rx antennas, as illustrated in the lower left of Figure 1 [24], [15]. The performance of such a bistatic L-band high-resolution wide-swath SAR system employing a planar antenna of 10 m x 0.65 m for radar pulse transmission and a reflector antenna with a dimeter of 12 m for radar echo reception is shown in Table 4. The case of using a reflector antenna with a diameter of 12 m also for radar pulse transmission has been investigated as well, reducing the required average Tx power to 188 W and improving the ambiguity suppression by several dB.

SAR System with Slow PRI Variation and Multiple Elevation Beams

The main drawback of a monostatic SAR with multiple elevation beams is the emergence of blind ranges which prevents the mapping of a wide swath without gaps. Over the last years, several solutions have been proposed to overcome this limitation. One option is a two-burst ScanSAR mode where each burst maps two or more swaths at the same time [15]. A detailed analysis of this mode revealed that the performance can be notably improved by using instead of two different pulse repetition frequencies a slowly varying pulse repetition interval as illustrated in Figure 1 on the lower middle left [8]. Several variants of such a system have been analysed within the ESA contract "Advanced Processing Techniques for Next Generation

Table 5: Performance of Reflector SAR with Slow PRI Variation

Parameter	Value	NESZ	Range Ambiguities (RASR)	Azimuth Ambiguities (AASR)
Antenna	12 m ∅	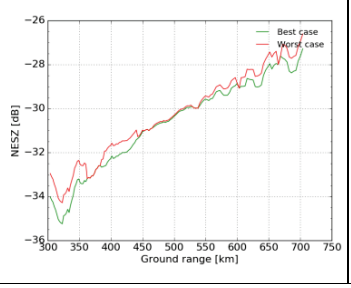	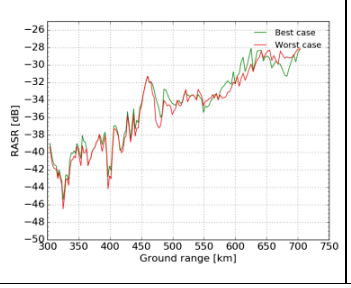	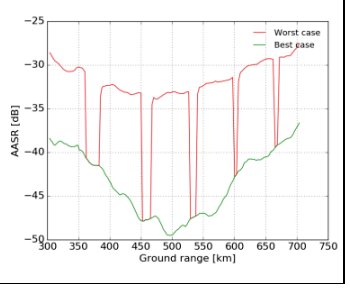
Orbit Alt.	773 km			
Elev. Ch.	45			
Az. Ch.	1			
Tx Power	883 W (avg.)			
Losses+NF	5.5 dB			
Duty Cycle	4%			

Table 6: Performance of Staggered SAR

Parameter	Value	NESZ	Range Ambiguities (RASR)	Azimuth Ambiguities (AASR)
Antenna	15 m ∅	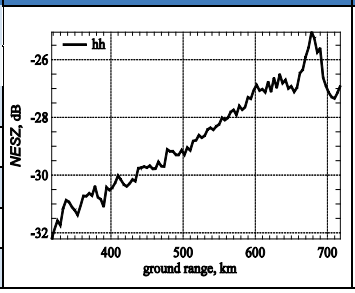	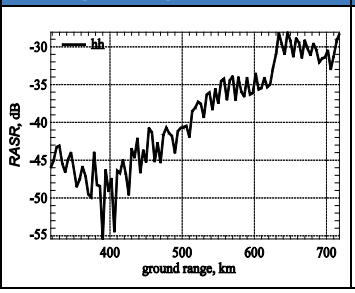	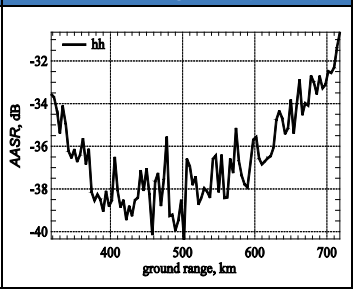
Orbit Alt.	773 km			
Elev. Ch.	50			
Az. Ch.	1			
Tx Power	306 W (avg.)			
Losses+NF	6.1 dB			
Duty Cycle	6%			

Multichannel SARs" and Table 5 shows the performance of one exemplary system configuration which uses a slow PRF variation from 3300 Hz to 3444 Hz within a cycle time of T_{cycle} = 3.54 s. The system operates with 80 MHz bandwidth and the NESZ is better than -26.6 dB for an average transmit power of 883 W. This means that an average Tx power of 610 W would be sufficient to satisfy the sensitivity requirement of NESZ ≤ -25 dB. The RASR is below -28.0 dB and the AASR is below -27.6 dB for an azimuth resolution that is always better than 5.05 m. The ambiguity performance can be improved by using not only one but multiple azimuth channels. A performance analysis with five azimuth channels reduced, for example, the AASR to -37.5 dB and the RASR to -30.6 dB. As also the NESZ improved to -28.0 dB, the average transmit power could be reduced to 440 W to still comply with the -25 dB NESZ sensitivity requirement. The use of multiple azimuth channels opens also the door to operate the system, for a reduced swath width, in different modes like a multi-channel staggered SAR which notably improves the azimuth resolution.

Staggered SAR

An alternative to the mode with the slow PRI variation is a fast variation of the PRI as conceptionally suggested in [25], [15] and elaborated in detail in [26], [27], [28]. This staggered SAR mode has also been selected as baseline for Tandem-L, which uses a deployable reflector with a diameter of 15 m in combination with a digital feed array [4], [29], [30]. As the staggered SAR mode has been described in detail in several other papers, we summarize in Table 6 only the results for the specific system design developed in this study. The NESZ varies between -32 dB and -25 dB, assuming an average radiated power of only 306 W. The range and azimuth ambiguities are also sufficiently low to meet the DTAR requirement of -25 dB from Table 1. A main advantage of the staggered SAR mode is that it is essentially an ultra-wide swath stripmap mode, which avoids the squint-angle discontinuities associated with the previous burst modes.

Multichannel Staggered SAR

The staggered SAR mode is a promising solution to map an ultra-wide swath of 400 km with an azimuth resolution of δ_{az} = 5 m which requires an effective aperture length in the order of $l_{ant} \approx 10$ m (ca. 15 m for a reflector). A higher azimuth resolution of, e.g., δ_{az} = 1 m would, however, require a rather short antenna in combination with very short pulse repetition intervals of less than 0.1 ms to avoid azimuth ambiguities. Hence, a very high antenna would be required to suppress range ambiguities. A similar range ambiguity challenge arises also in the quad-pol mode, where a detailed analysis revealed that the staggered SAR from the previous section cannot meet the DTAR requirements from Table 1 over the full 400 km wide swath in a fully polarimetric mode, especially as the weak cross-pol returns have to compete against the typically much stronger co-pol returns from adjacent Tx pulses. Such problems can be avoided by increasing the reflector size and adding additional feed elements in the azimuth direction. A new processing technique is, however, required to combine the staggered SAR mode with an antenna architecture that comprises multiple azimuth channels [31], [32]. Table 7 shows the resulting quad-pol performance of such a multichannel staggered SAR system which employs in this case an 18 m reflector. Assuming an average transmit power of 302 W, the NESZ is better than -25.5 dB which means that a power of only 267 W could fulfil the NESZ requirement even in quad-pol mode. This power value is remarkable, as it is the lowest of all analysed systems in this study, despite the operation in quad-pol mode. The system achieves this high sensitivity owing to the large reflector area. The worst-case RASR is below -27.2 dB in the cross-pol case, indicating that the performance goal is achieved over the desired 400 km swath. The AASR is below -34.5 dB over the full swath for an azimuth resolution (not shown) which even exceeds the 5.0 m requirement over the swath: the worst case is 4.4 m, leaving margin for spectral filtering (e.g. hamming).

Table 7: Performance of Multichannel Staggered SAR Operated in a Fully Polarimetric (Quad-Pol) Mode

Parameter	Value	NESZ	Range Ambiguities (RASR)	Azimuth Ambiguities (AASR)
Antenna	18 m ∅	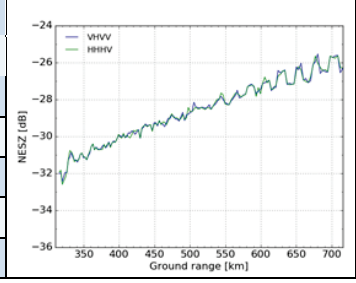	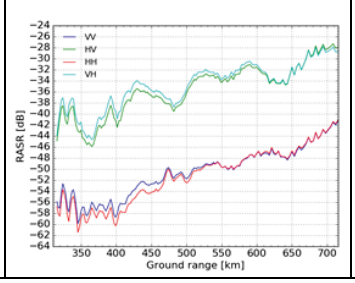	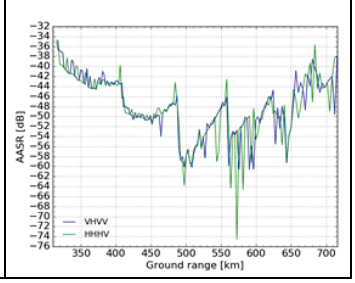
Orbit Alt.	773 km			
Elev. Ch.	65			
Az. Ch.	4			
Tx Power	302 W (avg.)			
Losses+NF	6.0 dB			
Duty Cycle	2+2%			

REFERENCES

[1] A. Moreira et al., "*A tutorial on synthetic aperture radar*," IEEE Geosc. Remote Sens. Mag., Vol.1, No. 1, pp.6–43, 2013.

[2] R. Torres et al., "*GMES Sentinel-1 mission*," Remote Sensing of Environment, Vol. 120, pp. 9–24, May 2012.

[3] M.J. Sanjuan-Ferrer et al., "*High Resolution Wide Swath SAR Applications Study: An Overview*," Proc. ARSI'14, Nov. 2014.

[4] A. Moreira et al., "*Tandem-L: A Highly Innovative Bistatic SAR Mission for Global Observation of Dynamic Processes on the Earth's Surface*," IEEE Geosci. Remote Sens. Magazine, Vol. 3, No. 2, pp. 8–23, 2015.

[5] A. Currie and M.A. Brown, "*Wide-swath SAR*," IEE Proc. for Radar and Signal Processing, Vol. 139, pp. 122–135, 1992.

[6] H.D. Griffiths and P. Mancini, "*Ambiguity suppression in SARs using adaptive array techniques,*" Proc. IGARSS, 1991.

[7] G.D. Callaghan, I.D. Longstaff, "*Wide-swath space-borne SAR using a quad-element array*," IEE Proceedings for Radar, Sonar and Navigation, Vol. 146, pp. 159-165, 1999.

[8] G. Krieger et al., "*SIMO and MIMO System Architectures for High-Resolution Ultra-Wide-Swath SAR Imaging*," European Conference on Synthetic Aperture Radar (EUSAR), Hamburg, Germany, 2016.

[9] J.H. Blythe, "*Radar Systems*," US Patent 4253098, issued February 24, 1981.

[10] M. Suess, B. Grafmueller, R. Zahn, "*A novel high resolution, wide swath SAR*," Proc. IGARSS, pp. 1013–1015, 2001.

[11] M. Younis, C. Fischer, W. Wiesbeck, "*Digital beamforming in SAR systems,*" IEEE Trans. Geosci. Rem. Sens., Vol. 41, 2003.

[12] G. Krieger, N. Gebert, A. Moreira, "*Multidimensional waveform encoding: A new digital beamforming technique for synthetic aperture radar remote sensing*," IEEE Transactions on Geoscience and Remote Sensing, Vol. 46, No. 1, pp. 31–46, 2008.

[13] G. Krieger, "*MIMO-SAR: Opportunities and pitfalls*," IEEE Trans. Geosci. Remote Sens., Vol. 52, pp. 2628–2645, 2014.

[14] J.-H. Kim, M. Younis, A. Moreira, W. Wiesbeck, "*Spaceborne MIMO synthetic aperture radar for multimodal operation*," IEEE Transactions on Geoscience and Remote Sensing, Vol. 53, No. 5, pp. 2453–2466, May 2015.

[15] G. Krieger, N. Gebert, M. Younis, F. Bordoni, A. Patyuchenko, A. Moreira, "*Advanced concepts for ultra-wide swath SAR imaging*," in Proc. European Conf. Synthetic Aperture Radar, Friedrichshafen, Germany, June 2008.

[16] M. Ludwig, C. H. Buck, S. D'Addio, R. Torres, F. Rostan, C. Schaefer, R. Croci, "*Earth observation instruments with e-scan antennas state-of-the-art and outlook,*" in Proc. IEEE MTT-S International Microwave Symposium, May 23–28, 2010.

[17] N. Gebert, G. Krieger, A. Moreira. "*Multichannel azimuth processing in ScanSAR and TOPS mode operation*," IEEE Transactions on Geoscience and Remote Sensing, Vol. 48, No. 7, pp. 2994–3008, July 2010.

[18] C. Schaefer, C. Heer, M. Ludwig, "*Advanced C-Band Instrument Based on Digital Beamforming*," EUSAR, Germany, 2010.

[19] M. Ludwig, M. Suess, N. Ayllon, G. Adamiuk, "*Digital beamforming for C-band SAR and technological elements*," in Proc. IEEE Geoscience and Remote Sensing Symposium (IGARSS), Milano, Italy, July 26-31, 2015.

[20] J.T. Kare, "*Moving receive beam method and apparatus for synthetic aperture radar*," US 6175326 B1, June 29, 1998.

[21] A. Freeman et al., "*SweepSAR: Beam-forming on receive using a reflector-phased array feed combination for spaceborne SAR*," in Proc. IEEE Radar Conference (RadarCon), Pasadena, USA, 2009.

[22] M. Younis, S. Huber, A. Patyuchenko, F. Bordoni, G. Krieger, "*Performance Comparison of Reflector- and Planar-Antenna Based Digital Beam-Forming SAR*", International Journal of Antennas and Propagation, 2009.

[23] S. Huber, M. Younis, A. Patyuchenko, G. Krieger, A. Moreira, "*Spaceborne Reflector SAR Systems with Digital Beam-forming*," IEEE Trans.Aerospace Electronic Systems, Vol. 48, pp. 3473-93, 2012.

[24] G. Krieger and A. Moreira, "*Potentials of digital beamforming in bi- and multistatic SAR*," in Proc. IEEE Geoscience and Remote Sensing Symposium, pp. 527-529, Toulouse, France, 2003.

[25] B. Grafmueller and C. Schaefer, "*High Resolution Synthetic Aperture Radar Device and Antenna for One Such Radar*", US 2009/0079621 A1.

[26] M. Villano, G. Krieger, A. Moreira, "*Staggered SAR: High-resolution wide-swath imaging by continuous PRI variation*," IEEE Transactions on Geoscience and Remote Sensing, Vol. 52, No. 7, pp. 4462–4479, July 2014.

[27] M. Villano, G. Krieger, A. Moreira, "*A Novel Processing Strategy for Staggered SAR*," IEEE Geoscience and Remote Sensing Letters, Vol. 11, No. 11, pp. 1891–1895, 2014.

[28] M. Villano, G. Krieger, A. Moreira, "*Staggered SAR: Performance Analysis and Experiments with Real Data*," IEEE Transactions on Geoscience and Remote Sensing, in print.

[29] S. Huber et al., "*Tandem-L: design concepts for a next-generation spaceborne SAR system*," Proc. EUSAR, June 2016.

[30] S. Huber et al., "*Tandem-L: A Technical Perspective on Future Spaceborne SAR Sensors for Earth Observation*," in revision

[31] F. Queiroz de Almeida and G. Krieger, "*Multichannel Staggered SAR Azimuth Sample Regularization*," European Conference on Synthetic Aperture Radar (EUSAR), Hamburg, Germany, June 2016.

[32] F. Queiroz de Almeida, M. Younis, G. Krieger, A. Moreira, "*Multichannel Staggered SAR Azimuth Processing*," in revision.

[33] F. Feng, S. Li, W. Yu, P. Huang, W. Xu, "*Echo separation in multidimensional waveform encoding SAR remote sensing using an advanced null-steering beamformer,*" IEEE Trans. Geosci. Remote Sens., Vol. 50, pp. 4157-72, 2012.

[34] F. He, X. Ma, Z. Dong, D. Liang, "*Digital beamforming on receive in elevation for multidimensional waveform encoding SAR sensing*," IEEE Geosci. Remote Sens. Letters, Vol. 11, pp. 2173-77, 2014.

[35] G. Krieger et al., "*CEBRAS: Cross elevation beam range ambiguity suppression for high-resolution wide-swath and MIMO SAR imaging,*" in Proc. IGARSS, July 2015.

[36] F. De Zan, P. Prats-Iraola, R. Scheiber, A. Rucci, "*Interferometry with TOPS: coregistration and azimuth shifts*", Proc. EUSAR, pp. 949-952, 3-5 June 2014.

[37] G. Krieger, F. De Zan, P. Lopez Dekker, J.S. Kim, M. Rodriguez-Cassola, A. Moreira, "*Impact of TEC gradients and higher-order ionospheric disturbances on spaceborne single-pass SAR interferometry,*" in Proc. IGARSS, July 2015.

[38] P. Prats et al., "*Demonstration of the applicability of 2-look burst modes in non-stationary scenarios with TerraSAR-X,*" Proc. EUSAR, June 2016.

[39] M. Villano, G. Krieger, A. Moreira, German patent application, Nr. 10 2017 205 649.5, 3. April 2017.